Evaluation of Different Calibration Approaches for JPSS CrIS

Yong Chen[1,2], and Yong Han[2]

Contact info: Yong.Chen@noaa.gov

[1]ESSIC, University of Maryland, College Park, MD 20740, USA

[2]NOAA/NESDIS Center for Satellite Applications and Research, College Park, MD 20740, USA

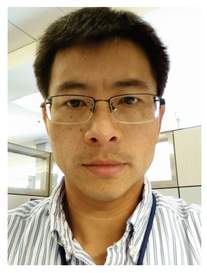

Abstract

The Cross-track Infrared Sounder (CrIS) on Suomi National Polar-orbiting Partnership Satellite (S-NPP) is a Fourier transform spectrometer and provides a total of 1305 and 2211 channels in normal mode and full spectral resolution (FSR) mode, respectively, for sounding the atmosphere. NOAA operated CrIS in FSR mode on December 4, 2014 for SNPP. Based on CrIS Algorithm Development Library (ADL), CrIS full resolution Processing System (CRPS) has been developed to generate the FSR Sensor Data Record (SDR). This code can also be run for normal mode and truncation mode SDRs.

Since CrIS is a Fourier transform spectrometer, the CrIS SDR need to be radiometrically and spectrally calibrated. The current calibration approach does the radiometric calibration first, and then applies the correction matrix operator (CMO), which includes the post calibration filter, spectral resampling, self-apodization removal and residual instrument line shape (ILS) removal, to the spectral calibration. In order to select the next calibration algorithm for CrIS on JPSS-1, four different calibration approaches are being implemented in the ADL full resolution code. In this study, evaluation results from these different calibration approaches are presented and the ringing effect observed in CrIS unapodized spectra are discussed.

CrIS Radiance Simulation

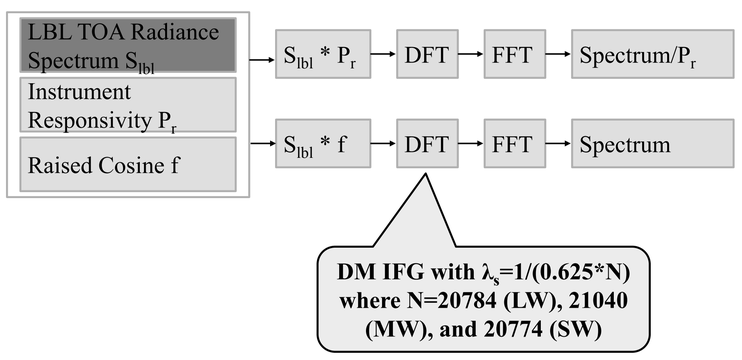

LBL truth spectra using responsivity and raised cosine filter at the band edge

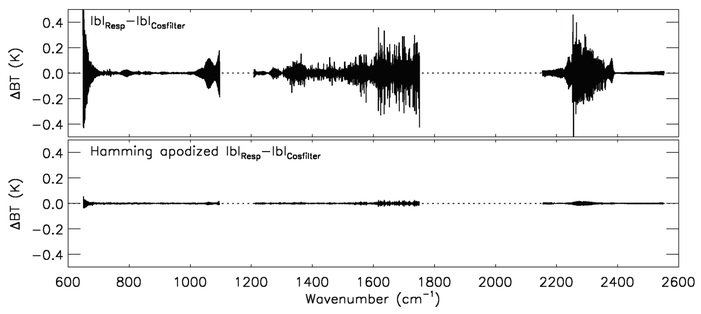

- LBLRTM version 12.2, with spacing at 0.001 cm^{-1} true LBL calculations, using matched ECMWF 3 hour forecast/analysis fields, spatially and temporally interpolated to observed time and location, convolved with CrIS instrument responsivity (Hank et al. 2014), and raised cosine filter through FFT to CrIS user grid.
- Significant differences occur at the beginning edge of band1 and the ending edge of band2
- When Hamming apodization is applied, the difference are very small (~0.02 K)

Calibration Approaches

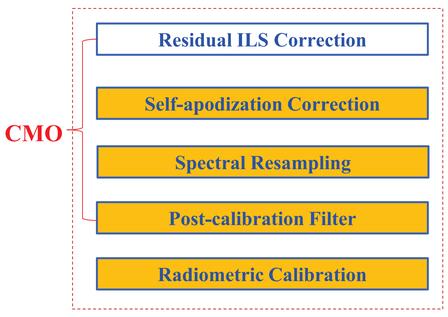

***R* – ILS residual;**
***SA* – Self-apodization;**
***F* – resampling;**
f_{ATBD} – post-filter

- Four calibration equations based on recommendation from CrIS science team are implemented in the CRPS
- An index in the ADL PCT file (configuration file) configures the code for a particular calibration equation

Calibration approaches supported by CRPS

Calibration algorithm 1 (the **baseline algorithm** delivered on January, 2015):

$$S_{Cal} = SA^{-1} \cdot F \cdot f_{ATBD} \cdot \{\frac{S_e - < S_{SP} >}{< S_{ICT} > - < S_{SP} >} B_{ICT}\}$$

SA^{-1} – computed with the large N and expansion factor 1.4 (LW), 1.6 (MW) and 2 (SW)
F – resampling matrix computed with large N
f – post-filter

Calibration algorithm 2 & 3: (proposed algorithm 2 in Mooney, D. (2014) algorithm list)

$$S_{Cal} = B_{ICT} \frac{F \cdot f_{ATBD} \cdot SA^{-1} \cdot f_{ATBD} \cdot FIR^{-1} \cdot (S_e - < S_{SP} >)}{F \cdot f_{ATBD} \cdot SA^{-1} \cdot f_{ATBD} \cdot FIR^{-1} \cdot (< S_{ICT} > - < S_{SP} >)}$$

Algorithm 2
SA^{-1} – Sincq, small N
F – Mooney (small N)
f – post-filter
IFGs are centered by adding Phase to spectra

Algorithm 3
SA^{-1} – Sincq, big N
F – Mooney (big N)
f – post-filter

Calibration algorithm 4 (proposed algorithm in Predina and Han (2015)):

$$S_{Cal} = B_{ICT} \frac{F \cdot f_{ATBD} \cdot SA^{-1} \cdot f_{ATBD} \cdot \{\frac{\Delta S_1}{\Delta S_2} |\Delta S_2|\}}{F \cdot f_{ATBD} \cdot SA^{-1} \cdot f_{ATBD} \cdot |\Delta S_2|}$$

$$\Delta S_1 = FIR^{-1}(S_e - < S_{SP} >)$$
$$\Delta S_2 = FIR^{-1}(< S_{ICT} > - < S_{SP} >)$$

SA^{-1} – Sincq, big N
F – Mooney (big N)
f – post-filter

Self-apodization matrix (SA)

Small N, (N): Number of bins after decimation	$SA[k',k] = \int_{\sigma_{min}}^{\sigma_{max}} \text{Psinc}(\frac{\sigma_{k'} - \sigma'}{\Delta\sigma_u}, N) ILS(\sigma', \sigma_k) d\sigma', \quad k = 0, N-1, k' = 0, N-1$	Expansion factor β=1.0 for all three bands
Big N, (N_0): Number of bins before decimation	$SA[k',k] = \int_{\sigma_{min}}^{\sigma_{max}} \text{Psinc}(\frac{\sigma_{k'} - \sigma'}{\Delta\sigma_u}, N_0) ILS(\sigma', \sigma_k) d\sigma', \quad k = 0, \beta N-1, k' = 0, \beta N-1$	Expansion factor β=1.4 (LW), 1.6 (MW) and 2.0 (SW), respectively

Resampling matrix (F)

Small N, (N): Number of bins after decimation	$F[k,k'] = \frac{\Delta\sigma_z}{\Delta\sigma_u} \frac{Sin(\pi \frac{\sigma_{z,k'} - \sigma_{u,k}}{\Delta\sigma_u})}{NSin(\pi \frac{\sigma_{z,k'} - \sigma_{u,k}}{N\Delta\sigma_u})}, \quad k = 0, N-1; k' = 0, N-1$
Big N, (N_0): Number of bins before decimation	$F[k,k'] = \frac{\Delta\sigma_z}{\Delta\sigma_u} \frac{Sin(\pi \frac{\sigma_{z,k'} - \sigma_{u,k}}{\Delta\sigma_u})}{N_0 Sin(\pi \frac{\sigma_{z,k'} - \sigma_{u,k}}{N_0\Delta\sigma_u})}, \quad k = 0, N-1; k' = 0, N-1$

SDR Radiance Direct Comparison Results

LW sweep direction differences (ringing) $(BT_{obs})_{fwd} - (BT_{obs})_{rev}$

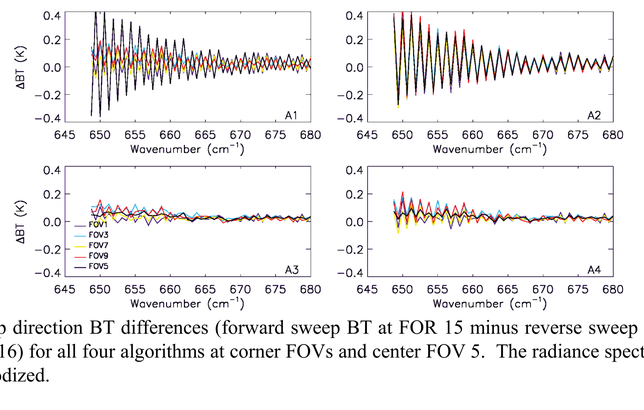

Sweep direction BT differences (forward sweep BT at FOR 15 minus reverse sweep BT at FOR 16) for all four algorithms at corner FOVs and center FOV 5. The radiance spectra are unapodized.

Mean BT difference between algorithms

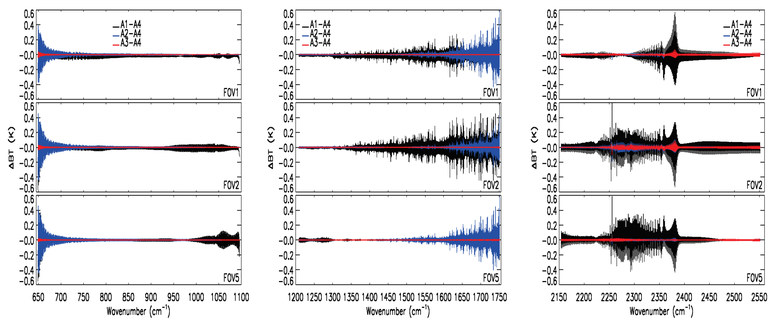

Mean brightness temperature differences between other algorithms (1, 2, and 3) and algorithm 4 for LWIR (left panel), MWIR (middle panel), and SWIR (right panel) at FOVs 1, 2, and 5. The radiance spectra are unapodized.

- Algorithms 3 and 4 significantly reduce the sweep direction differences especially for FOV 5 at the beginning edge of band 1; larger ringing artifacts are showed in Algorithms 1 and 2
- The mean BT differences between other algorithms and algorithm 4 show: For LW, Algorithm 1 has larger difference at the both band edges; Algorithm 2 only has large difference at the beginning of the band edge. For MW, Algorithms 1 and 2 have larger differences towards the end of band. For SW Algorithms 1 has larger differences at the coldest lines and regions. For all bands, Algorithm 3 is basically the same as Algorithm 4.

SDR Radiance Compared with LBL Simulation

A4 compared with different LBL truths

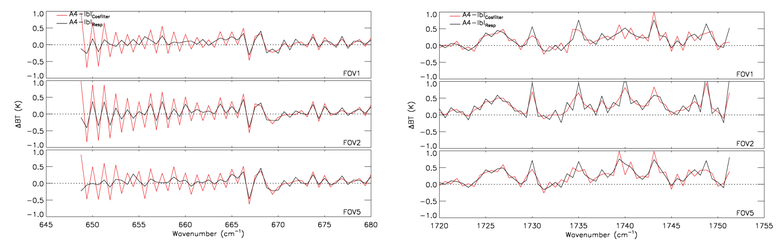

- A4 minus lbl_{Resp} gives the best results for all FOVs at LWIR band, and mixed results at MWIR band compared to A4 minus $lbl_{CosFilter}$. In this study, we use lbl_{Resp} as truth spectra.

Sweep direction differences (ringing) $(BT_{obs} - BT_{lbl})_{fwd} - (BT_{obs} - BT_{lbl})_{rev}$

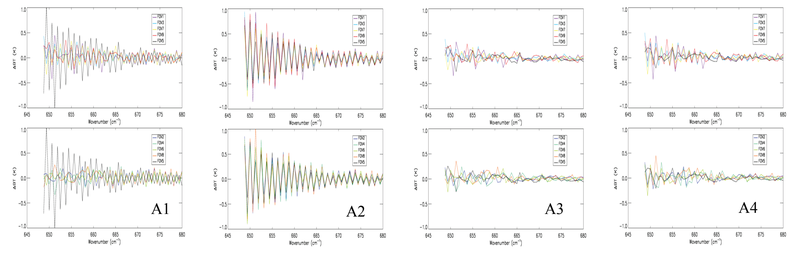

Calibration bias using LBLRTM simulation $BT_{obs} - BT_{lbl}$

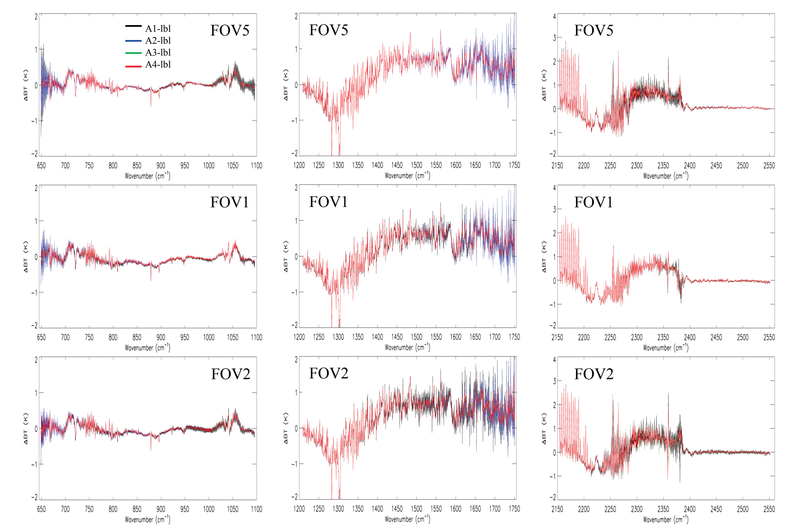

Mean brightness temperature differences between observations in SDR from the four algorithms and Line-by-Line simulation over clear ocean scenes. The radiance spectra are unapodized.

FOV-2-FOV comparison $(BT_{obs} - BT_{lbl})_{fov\_i} - (BT_{obs} - BT_{lbl})_{fov\_5}$

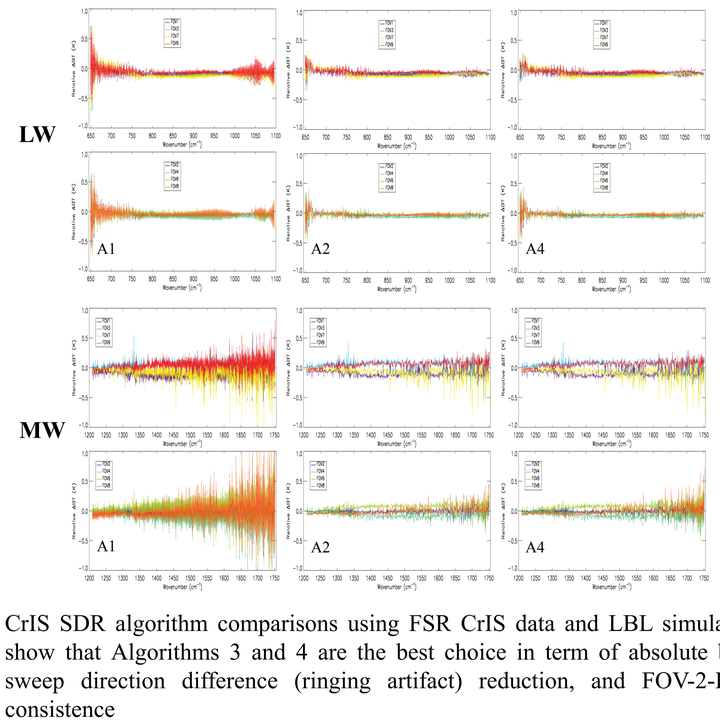

- CrIS SDR algorithm comparisons using FSR CrIS data and LBL simulation show that Algorithms 3 and 4 are the best choice in term of absolute bias, sweep direction difference (ringing artifact) reduction, and FOV-2-FOV consistence

Conclusion

- In this study, we have implemented different calibration approaches in the CrIS full resolution SDR code in order to study the ringing effect observed in CrIS unapodized spectra and to support to select the best calibration algorithm for J1
- Results show Algorithms 3 and 4 are the best choice in term of absolute bias, sweep direction difference (ringing artifact) reduction, and FOV-2-FOV consistence
- Based on these results, we strongly recommend that Algorithm 4 as the J1 calibration algorithm to implement into J1 CrIS code since Algorithm 4 is more computationally efficient than Algorithm 3

References and Acknowledgments

- Han, Y., et al. (2013), Suomi-NPP CrIS measurements, sensor data record algorithm, calibration and validation activities, and record data quality, *J. Geophys. Res. Atmos.*, 118, doi:10.1002/2013JD020344
- Mooney, D. (2014), CrIS Calibration Equation, *STAR JPSS Annual Science Team Meeting*, May 12-16, 2014, College Park, MD
- Predina, J. and Han, Y. (2015), Alternate CrIS SDR Algorithm Flows. February 25, 2015, *CrIS SDR Science Team meeting*
- Revercomb, H., et al. (2014), CrIS Ringing Artifact: Root Cause Confirmation and Approach to Removal. March 12, 2014, *CrIS SDR Science Team meeting*

The Authors would like to extend their thanks to the S-NPP CrIS SDR Science Team for their valuable contributions.